

## NOTES AND CORRESPONDENCE

**The Effects of the Full Coriolis Force on the Structure and Motion of a Tropical Cyclone. Part I: Effects due to Vertical Motion**

XUDONG LIANG

*Shanghai Typhoon Institute, China Meteorological Administration, Shanghai, China*

JOHNNY C. L. CHAN

*Shanghai Typhoon Institute, China Meteorological Administration, Shanghai, and Laboratory for Atmospheric Research, Department of Physics and Materials Science, City University of Hong Kong, Hong Kong, China*

(Manuscript received 3 March 2004, in final form 17 February 2005)

## ABSTRACT

In most dynamical studies of synoptic-scale phenomena, only the components of the Coriolis force contributed by the horizontal motion are considered, and only in the horizontal momentum equation. The other components are neglected based on a scale analysis. However, it is shown that such an analysis may not be fully valid in a tropical cyclone (TC) and that these terms should be included. The two neglected terms are 1)  $e_w$ , the Coriolis force in the  $x$ -momentum equation due to vertical motion, and 2)  $w_e$ , the Coriolis force in the vertical equation of motion due to the zonal wind. In this paper, effects of the first term (i.e.,  $e_w$ ) on the structure and motion of a TC are investigated through numerical simulations using the fifth-generation Pennsylvania State University–National Center for Atmospheric Research (PSU–NCAR) Mesoscale Model (MM5).

The results suggest that after the  $e_w$  term has been included, the structure of a TC even on an  $f$  plane is changed. A southwestward displacement of a TC center with a speed of  $\sim 1 \text{ km h}^{-1}$  is found in the  $f$ -plane experiment. On a  $\beta$  plane, inclusion of the  $e_w$  term gives a vortex track that is generally west to southwest of the inherent northwestward track (due to the  $\beta$  effect). A scale analysis suggests that the  $e_w$  term can be as large as half the magnitude of the horizontal acceleration. This term generates an asymmetric wind structure with a generally easterly flow near the center, which therefore causes the vortex to displace toward the southwest. A rainfall asymmetry consistent with the convergence associated with the wind asymmetry is also found and accounts for 10%–20% of the symmetric parts.

**1. Introduction**

Scale analysis of synoptic-scale phenomena (Holton 1992) suggests that the only significant contribution of the Coriolis force to atmospheric flow is the Coriolis parameter  $f$  ( $= 2\Omega \sin\phi$ , where  $\Omega$  is the magnitude of the angular velocity of the earth and  $\phi$  is the latitude) multiplied by the horizontal wind vector, and only in the horizontal momentum equation. During the past two decades, studies on the motion of tropical cyclones (TCs) have generally concentrated on the so-called beta effect, which is due to the variation of  $f$  with latitude (see review in Elsberry 1995). Some asymmetric

structures and intensity changes of TCs have also been explained in terms of this effect (e.g., Madala and Piacsek 1975; Bender 1997; Peng et al. 1999).

In addition to this term, the full Coriolis force consists of two other terms: 1)  $e_w$  ( $= 2\Omega w \cos\phi$ ), the Coriolis force in the  $x$ -momentum equation due to the vertical motion  $w$ , and 2)  $w_e$  ( $= 2\Omega u \cos\phi$ ), the Coriolis force in the vertical momentum equation due to the zonal wind  $u$ . Holton (1992) suggested that since for midlatitude synoptic-scale weather systems,  $w$  is  $\sim 1 \text{ cm s}^{-1}$ ,  $e_w \sim 10^{-6} \text{ m s}^{-2}$  and can therefore be neglected when compared with the other terms in the  $x$ -momentum equation. However, according to observation studies (e.g., Gray 1965; Marks and Houze 1987; Black et al. 1996; Franklin et al. 1988), updrafts in the TC eyewall areas have average speeds of  $> 1 \text{ m s}^{-1}$ , with the peak value even  $> 10 \text{ m s}^{-1}$ . If  $w$  is  $\sim 1\text{--}10 \text{ m s}^{-1}$ ,  $e_w \sim 10^{-5}$  to  $10^{-4}$

Corresponding author address: Xudong Liang, Shanghai Typhoon Institute, 166 Puxi Rd., Shanghai 200030, China.  
E-mail: liangxd@mail.typhoon.gov.cn

$\text{m s}^{-2}$ , which will then be comparable to the acceleration term and should therefore be included in the equation. In nonhydrostatic numerical models and in the real atmosphere, vertical acceleration exists, which could be as large as  $\sim 10^{-4} \text{ m s}^{-2}$  near the TC eyewall, and is thus of the same order of magnitude as that of  $w_e$ . In other words, these two extra terms should be included in high-resolution numerical simulations related to TC studies.

The objective of this study is therefore to investigate the effect of the  $e_w$  term on the simulated structure and motion of TCs based on the fifth-generation Pennsylvania State University–National Center for Atmospheric Research (PSU–NCAR) Mesoscale Model (MM5). The effect of the  $w_e$  term will be discussed in a future paper. The model configuration is briefly described in section 2 together with the experiments to be conducted. To demonstrate the significance of the  $e_w$  term, a scale analysis of the various terms from the control run is carried out in section 3. The basic results of the experiments are presented in section 4. The mechanisms through which the  $e_w$  term modifies the structure and motion of a TC are examined in section 5. The results are then summarized and discussed in section 6.

## 2. Model and initial conditions

Version 3.4 of MM5 is used in this study, with a coarse domain of  $301 \times 301$  grid points having a grid spacing of 25 km and a two-way interactive inner domain of  $109 \times 109$  grid points having a horizontal resolution of 8.3 km. The terrain height is set to zero and the land-use category is set to the water bodies. The vertical coordinate consists of 21  $\sigma$  levels: 0.995, 0.98, 0.955, 0.92, 0.88, 0.835, 0.78, 0.72, 0.66, 0.60, 0.54, 0.48, 0.42, 0.36, 0.30, 0.24, 0.18, 0.25, 0.08, 0.045, and 0.015. All experiments are run with  $\phi = 20^\circ\text{N}$ . Physical processes include the Betts–Miller cumulus parameterization scheme (Betts and Miller 1993), simple ice explicit moisture scheme, and a high-resolution Blackadar planetary boundary layer scheme (Blackadar 1979) in the coarse-domain and mixed-phase explicit moisture without cumulus parameterization scheme in the inner domain. All the analyses are based on the output of the inner domain.

The initial conditions of all experiments consist of a prespecified vortex and a quiescent atmospheric environment, which are the same as those in Chan et al. (2001). Specifically, the vertical temperature structure of the environment is obtained from the reanalysis data of the European Centre for Medium-Range Weather Forecasts (ECMWF; 0000 UTC 21 September 1990)

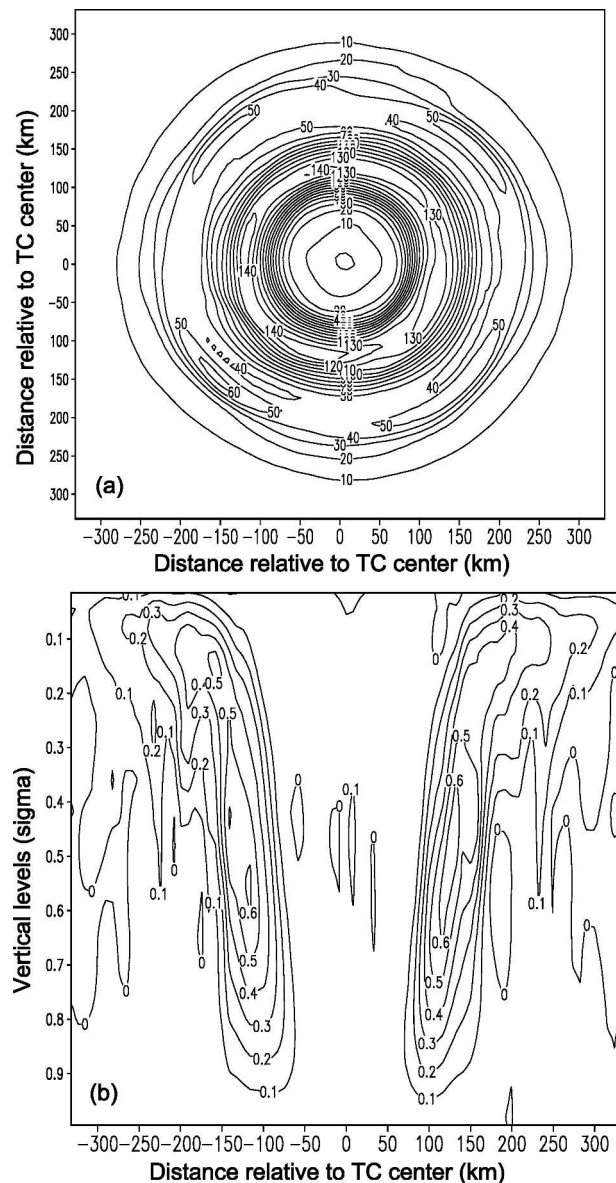


FIG. 1. (a) Accumulated 72-h rainfall (cm) and (b) vertical motion ( $\text{m s}^{-1}$ ) averaged between 0 and 72 h in the control run. The x axis is the distance relative to initial TC center in km. The y axis is as same as the x axis in (a) and its vertical sigma level in (b).

averaged within  $10^\circ\text{--}20^\circ\text{N}$ ,  $135^\circ\text{--}155^\circ\text{E}$ . Because the humidity values from the ECWMF reanalysis are too dry for the model TC to grow, these values are set to 90%, 85%, 80%, 50%, 20%, 20%, and 10% at the standard pressure levels from 1000 to 100 hPa, respectively. The geopotential heights at various pressure levels are calculated using the hydrostatic relationship. A TC vortex with a minimum sea level pressure (MSLP) of 980 hPa and a radius of  $15 \text{ m s}^{-1}$  winds of 250 km is inserted into the initial fields.

All experiments are integrated for 72 h. To eliminate

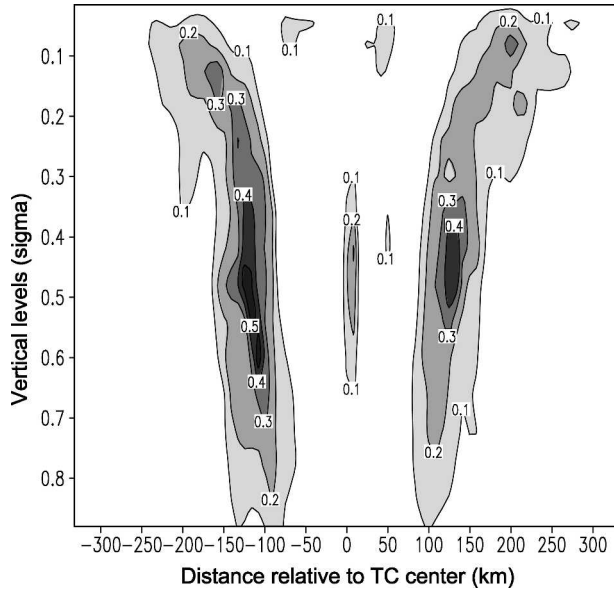


FIG. 2. As in Fig. 1b except for a south-north vertical cross section through the TC center of the ratio of  $e_w$  to the horizontal acceleration term in the control run averaged over 72 h.

the instantaneous variation of the fields, the precipitation, vorticity, and wind fields in a subdomain of  $81 \times 81$  grid points centered on the TC are selected and time averaged over 72 h based on the integration output every 1 h. All analyses of the various fields are based on these 1-h averages.

Four experiments are carried out, namely, on an  $f$  plane without the  $e_w$  term (control run), on an  $f$  plane with the  $e_w$  term included (the  $e_w$  experiment), on a  $\beta$  plane without the  $e_w$  term (the  $\beta$  experiment), and on a

$\beta$  plane with the  $e_w$  term included (the  $\beta_{ew}$  experiment). As expected, the accumulated rainfall is fairly symmetric (Fig. 1a) in the control run and the vortex center shows no significant displacement during the integration (not shown).

### 3. Scale analysis based on the control run results

Before analyzing the results of the experiments, it would be useful to examine the scale of the  $e_w$  term relative to the horizontal acceleration using the results from the control run to ascertain the extent of its contribution. As shown in Fig. 1b,  $w \sim 0.5 \text{ m s}^{-1}$  in the eyewall areas so that  $e_w (= 2\Omega w \cos\phi) \sim 10^{-4} \text{ m s}^{-2}$ , where  $\Omega = 7.292 \times 10^{-5} \text{ rad s}^{-1}$  and  $\phi = 20^\circ\text{N}$ . Using the output from the control run every 6 h, the horizontal acceleration can also be estimated. The ratio of  $e_w$  to the horizontal acceleration averaged over 72 h within the eyewall is found to be as large as 0.5 (Fig. 2), and thus the  $e_w$  term cannot be ignored.

### 4. Basic results from the $e_w$ and $\beta_{ew}$ experiments

Including the  $e_w$  term on an  $f$  plane (the  $e_w$  experiment) gives an asymmetric structure in the total rainfall (Fig. 3a), with that in the northeastern (southwestern) quadrant being enhanced (weakened; Fig. 3b). The total rainfall in the eyewall is  $\sim 100 \text{ cm}$ , and the asymmetric part is  $\sim 10\text{--}20 \text{ cm}$ , or  $\sim 10\%\text{--}20\%$  of the symmetric part. A northwestward then southwestward displacement is also observed (Fig. 4a). By 72 h, the vortex is  $\sim 80 \text{ km}$  (which gives an average displacement speed of  $\sim 0.3 \text{ m s}^{-1}$ ) to the southwest of the initial position.

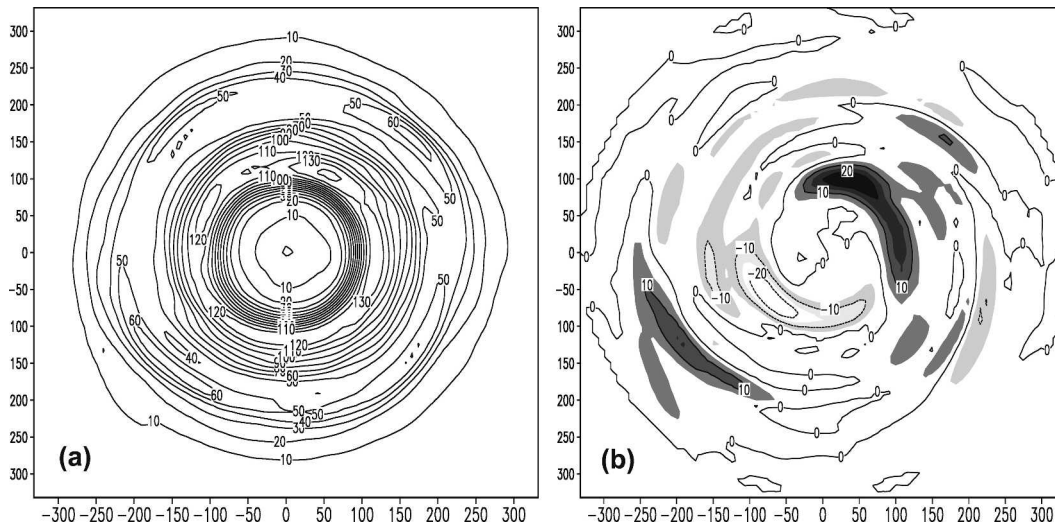


FIG. 3. Accumulated 72-h (a) total and (b) asymmetric precipitation in the  $e_w$  expt (cm).

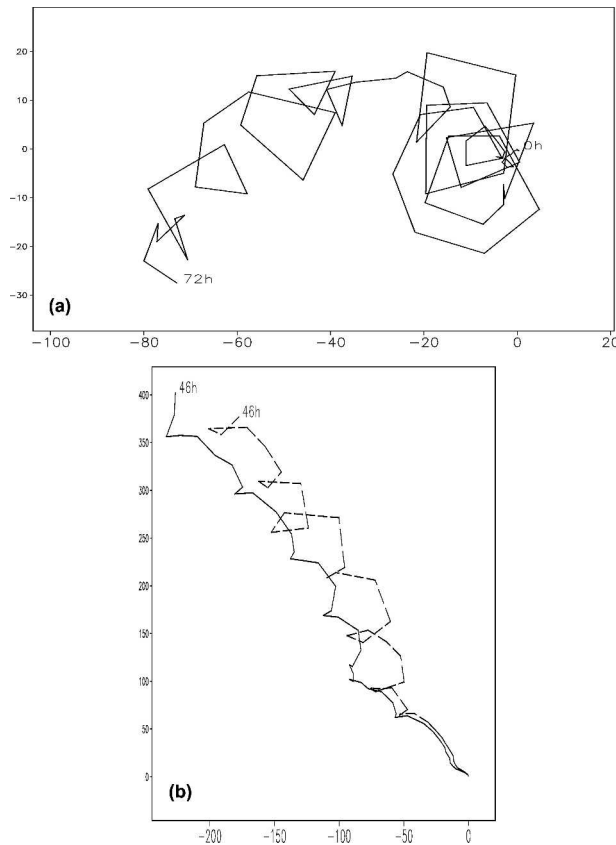


FIG. 4. Displacement of the TC center (a) from 0 to 72 h on an  $f$  plane for the  $e_w$  expt, and (b) from 0 to 46 h on a  $\beta$  plane for the  $\beta$  expt (dashed) and the  $\beta_{ew}$  expt (solid). The  $x$  and  $y$  axes are distances (km) relative to initial TC center.

However, no obvious difference in TC intensity between the control run and the  $e_w$  experiment can be found after 72 h of integration (Fig. 5).

In the  $\beta$  experiment, as expected, the rainfall distributions are also asymmetric (not shown) and, the TC moves northwestward with a speed of  $\sim 2.7 \text{ m s}^{-1}$  due to the  $\beta$  effect (Chan and Williams 1987; Fig. 4b). When the  $e_w$  term is included on the  $\beta$  plane (the  $\beta_{ew}$  experiment), the TC also moves northwestward but the track generally deviates to the west or southwest of that in the  $\beta$  experiment after  $\sim 20$  h integration. The deviation is  $\sim 50$  km after 46 h (the vortex moves out the inner domain after 46 h). Note again from Fig. 5 that the intensity of the TC in either experiment on a  $\beta$  plane does not differ much from that of the control.

## 5. Asymmetric structures and physical mechanism

To understand how the  $e_w$  term modifies the structure and movement of a TC, the results from the control run are first analyzed. The vorticity tendency con-

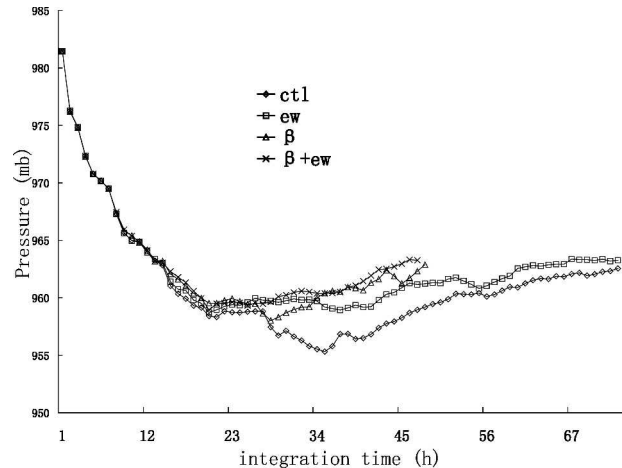


FIG. 5. Temporal variations of the MSLP in the four experiments. Ctl (control),  $e_w$ ,  $\beta$ , and  $\beta + e_w$  ( $\beta_{ew}$ ).

tributed by the  $e_w$  term is  $e(\partial w/\partial y)$ , which for simplicity will be referred to as the  $\gamma$  term hereafter. It is obvious from the eyewall structure in Fig. 1a that north of the TC center, this term must be positive (negative) inside (outside) the eyewall but with a reverse distribution south of the TC center, which is indeed the case based on the calculation from the vertical motion field (Fig. 6a). Because of the strong rising motion within the eyewall (see Fig. 1b), such a horizontal distribution of the  $\gamma$  term is found at all levels (Fig. 6b).

Consider the vorticity equation. If the vortex is symmetric, the only contribution to the asymmetric component of the vorticity tendency term (which is responsible for any displacement of the vortex) on an  $f$  plane is from the  $\gamma$  term. Because the positive (negative) area south (north) of the eyewall is more extensive, the net adjustment of the wind to this vorticity tendency distribution is to set up a pair of gyres (“ $\gamma$  gyres”), with anticyclonic flow to the north and cyclonic flow to the south, which produces a generally easterly flow across the TC center. This is indeed the case for the  $e_w$  experiment (Fig. 7), which can therefore explain the westward movement of the vortex. Note also the convergence (divergence) to the northeast (southwest) of the vortex, which is consistent with the asymmetric rainfall distribution shown in Fig. 3. In addition, the  $\gamma$  gyres cover a large area outside the eyewall, extending  $\sim 500$  km beyond the TC center (Fig. 7).

On a  $\beta$  plane, the situation is more complicated because the  $\beta$  effect itself produces an asymmetry in vertical motion (e.g., Peng et al. 1999). However, the magnitude of the  $\partial w/\partial y$  term would still be appreciable and would produce similar modifications to the asymmetric flow, and thus the deviations in the track shown in Fig. 4. However, due to asymmetries introduced by  $\beta$ , the



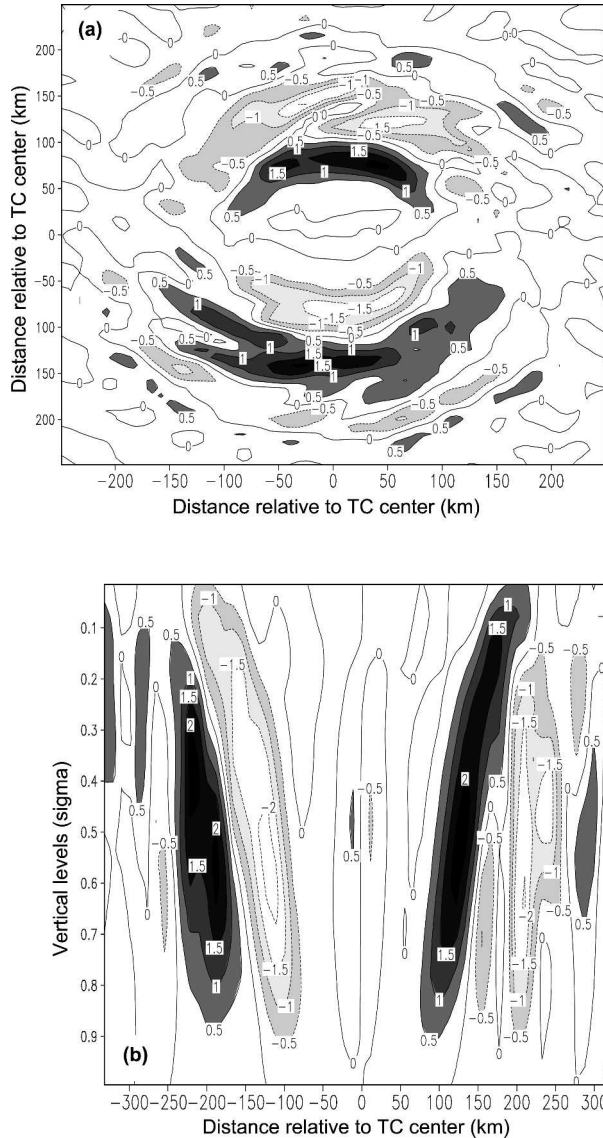


FIG. 6. As in Fig. 1 except for the  $e\partial w/\partial y$  term ( $10^{-9} \text{ s}^{-2}$ ) calculated using the averaged vertical velocity in Fig. 1b on the (a)  $\sigma = 0.72$  surface, and (b) south–north vertical cross section.

track deviations vary to northwest instead of southwest in the  $e_w$  experiment.

**6. Summary and conclusions**

Traditionally, the terms  $2\Omega w \cos\phi$  ( $e_w$ , Coriolis force due to vertical motion) in the  $x$ -momentum equation and  $2\Omega u \cos\phi$  ( $w_e$ , Coriolis force due to the zonal wind) in the vertical momentum equation have been neglected in studying midlatitude synoptic systems based on a scale analysis. However, because strong vertical motion and horizontal winds exist in the interior areas

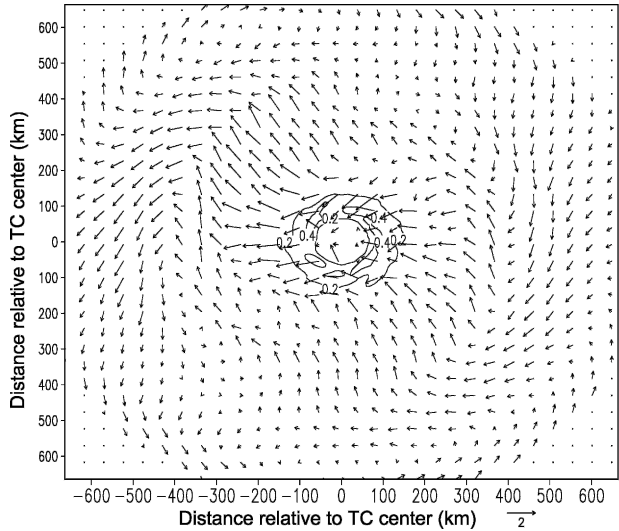


FIG. 7. The 72-h-averaged asymmetric winds (vectors) and upward motion (contour,  $\text{m s}^{-1}$ ) in the  $e_w$  expt.

of a tropical cyclone (TC), these terms may be important. This study represents an attempt to examine the extent to which the  $e_w$  term can modify TC structure and motion on both  $f$  and  $\beta$  planes.

The experiments using the fifth-generation Pennsylvania State University–National Center for Atmospheric Research (NCEP–NCAR) Mesoscale Model (MM5) indicate that on an  $f$  plane, inclusion of the  $e_w$  term enhances (reduces) the precipitation in the northeastern (southwestern) section of the TC. The amplitude of the asymmetry can be up to 10%–20% of the symmetric part. The TC also has a generally westward to southwestward displacement so that after 72 h, the vortex is  $\sim 80$  km to the southwest of the original position. On a  $\beta$  plane, the TC track in the experiment with inclusion of the  $e_w$  term deviates to the west-southwest from that without by  $\sim 50$  km after 46 h.

To demonstrate the significance of the  $e_w$  term, a scale analysis is performed using the results from the control run. It is found that within the eyewall areas of the TC, the ratio of  $e_w$  to the magnitude of the horizontal acceleration can be up to 0.5. The strong meridional gradient across the TC of the vertical motion within the eyewall gives rise to vorticity tendency asymmetries such that a generally easterly flow is generated. It is this easterly flow that causes the vortex to move westward. Asymmetries in this flow can also explain those in the rainfall observed in the experiments.

To summarize, this paper has shown that in the modeling of TCs, the component of the Coriolis force in the horizontal momentum equation due to vertical motion should not be neglected, especially in the study of the structure and motion of TCs. However, it appears that

this term has no appreciable effect on the intensity of a TC, despite changes in the precipitation distribution. The next step in this investigation will be the examination of the effect of the other component of the full Coriolis force (i.e., in the vertical momentum equation due to the effect of the zonal wind).

*Acknowledgments.* The authors thank the reviewers for their constructive comments on the first version of the manuscript, especially Dr. Mike Fiorino who provided a detailed conceptual comparison between the beta and the gamma terms. This research was supported by the National Natural Science Foundation of China Grants 40275018 and 40333025 and by the City University of Hong Kong Grant 7010010.

#### REFERENCES

- Bender, M. A., 1997: The effect of relative flow on the asymmetric structure in the interior of hurricanes. *J. Atmos. Sci.*, **54**, 703–724.
- Betts, A. K., and M. J. Miller, 1993: The Betts–Miller scheme. *The Representation of Cumulus Convection in Numerical Models, Meteor. Monogr.*, No. 46, Amer. Meteor. Soc., 107–121.
- Black, M. L., R. W. Burpee, and F. D. Marks Jr., 1996: Vertical motion characteristics of tropical cyclones determined with airborne Doppler radial velocities. *J. Atmos. Sci.*, **53**, 1887–1909.
- Blackadar, A. K., 1979: High resolution models of the planetary boundary layer. *Advances in Environmental Science and Engineering*, J. Pfafflin and E. Ziegler, Eds., Vol. 1, Gordon and Breach, 50–85.
- Chan, J. C.-L., and R. T. Williams, 1987: Analytical and numerical studies of the beta-effect in tropical cyclone motion. Part I: Zero mean flow. *J. Atmos. Sci.*, **44**, 1257–1265.
- , Y. Duan, and L. K. Shay, 2001: Tropical cyclone intensity change from a simple ocean–atmosphere coupled model. *J. Atmos. Sci.*, **58**, 154–172.
- Elsberry, R. L., Ed., 1995: Global perspectives of tropical cyclones. WMO/TD-693, Rep. TCP-38, World Meteorological Organization, 289 pp.
- Franklin, J. L., S. J. Lord, and F. D. Marks Jr., 1988: Dropwindsonde and radar observations of the eye of Hurricane Gloria (1985). *Mon. Wea. Rev.*, **116**, 1237–1244.
- Gray, W. M., 1965: Calculations of cumulus vertical draft velocities in hurricanes from aircraft observations. *J. Appl. Meteor.*, **4**, 463–474.
- Holton, J. R., 1992: *An Introduction to Dynamic Meteorology*. 3d ed. Academic Press, 511 pp.
- Madala, R. V., and S. A. Piacsek, 1975: Numerical simulation of asymmetric hurricanes on a beta-plane with vertical shear. *Tellus*, **27**, 453–468.
- Marks, F. D., Jr., and R. A. Houze Jr., 1987: Inner-core structure of Hurricane Alicia from airborne Doppler radar observations. *J. Atmos. Sci.*, **44**, 1296–1317.
- Peng, M. S., B.-F. Jeng, and R. T. Williams, 1999: A numerical study on tropical cyclone intensification. Part I: Beta effect and mean flow effect. *J. Atmos. Sci.*, **56**, 1404–1424.